

# Analysis of Reliability Dynamics of SSD RAID (Supplementary File)

Yongkun Li, *Member, IEEE* Patrick P. C. Lee, *Member, IEEE* John C. S. Lui, *Fellow, IEEE*



## 1 PROOF OF THEOREM 1 IN §3.1 OF THE MAIN PAPER

Based on the definition of error  $\epsilon_l$ , we have

$$\epsilon_l = \|\hat{\pi}((l+1)sT) - \tilde{\pi}((l+1)sT)\|_1. \quad (1)$$

Note that  $\tilde{\pi}((l+1)sT)$  and  $\hat{\pi}((l+1)sT)$  are computed by Equation (11) and Equation (12) in §3.1 of the main paper, respectively. So we can rewrite error  $\epsilon_l$  as follows.

$$\begin{aligned} \epsilon_l &= \|\hat{\pi}(lsT)e^{-\tilde{\Lambda}_l sT}e^{\tilde{\Lambda}_l sT}\tilde{P}_l^n - \tilde{\pi}(lsT)e^{-\tilde{\Lambda}_l sT}e^{\tilde{\Lambda}_l sT}\tilde{P}_l^n \\ &\quad - \hat{\pi}(lsT)\sum_{n=U_l+1}^{\infty} e^{-\tilde{\Lambda}_l sT} \frac{(\tilde{\Lambda}_l sT)^n}{n!} \tilde{P}_l^n\|_1 \end{aligned}$$

Now, we can bound the error  $\epsilon_l$  as follows.

$$\begin{aligned} \epsilon_l &\leq \|\hat{\pi}(lsT) - \tilde{\pi}(lsT)\|_1 e^{-\tilde{\Lambda}_l sT} e^{\tilde{\Lambda}_l sT} \|\tilde{P}_l\|_{\infty} \\ &\quad + \|\hat{\pi}(lsT)\sum_{n=U_l+1}^{\infty} e^{-\tilde{\Lambda}_l sT} \frac{(\tilde{\Lambda}_l sT)^n}{n!} \tilde{P}_l^n\|_1 \\ &= \epsilon_{l-1} + \left(1 - \sum_{n=0}^{U_l} e^{-\tilde{\Lambda}_l sT} \frac{(\tilde{\Lambda}_l sT)^n}{n!}\right). \end{aligned}$$

The last equation comes from the fact that  $\|\tilde{P}_l\|_{\infty} = 1$  as  $\tilde{P}_l = \mathbf{I} + \frac{\tilde{Q}_l}{\tilde{\Lambda}_l}$ , and  $\epsilon_{l-1} = \|\hat{\pi}(lsT) - \tilde{\pi}(lsT)\|_1$ . Therefore, we have the results stated in Theorem 1. ■

## 2 PROOF OF THEOREM 2 IN §3.2 OF THE MAIN PAPER

Note that the error rate of one stripe is a monotonically increasing function of system age  $k$  in each interval as we stated in §3.2 of the main paper. Therefore, considering the  $s$  time periods in each interval, error rate in the first period must be the smallest, and that in the last time period is the largest.

Note that as shown in Figure 1, if error rate increases, then the rate of the transition from a state with small state number to a state with big state number increases, i.e.,  $q_{i,i+1}(k)$  increases, while the rate of opposite transitions, i.e.,  $q_{i,i-1}(k)$ , keeps unchanged. Moreover, when

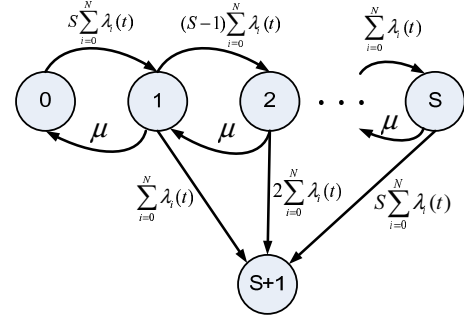


Fig. 1: State transition of the non-homogeneous CTMC.

state number  $i$  increases, the transition rate to state  $S+1$ , i.e.,  $q_{i,S+1}(k)$ , also increases. Therefore, if error rate gets increased, then the system will transit to the state of data loss with higher chance.

Therefore, if the error rate in each of the  $s$  time periods in each interval is set as the one in the first time period, i.e., let  $\tilde{Q}_l = Q_{l_s}$ , then the RAID reliability must be overestimated. Correspondingly, if we let  $\tilde{Q}_l = Q_{l_{s+s-1}}$ , then the RAID reliability must be underestimated. Mathematically, if we denote  $R(t)$  as the accurate solution, and denote  $R_1(t)$  and  $R_2(t)$  as the solutions in the cases where  $\tilde{Q}_l = Q_{l_{s+s-1}}$  and  $\tilde{Q}_l = Q_{l_s}$  respectively, then we have  $R_1(t) \leq R(t) \leq R_2(t)$  as shown in the theorem. ■

## 3 PROOF OF COROLLARY 1 IN §3.2 OF THE MAIN PAPER

As stated before, for each interval  $(lsT, (l+1)sT)$ , error rate in the  $s$  consecutive time periods is monotone increasing. Therefore, for any generator matrix  $\tilde{Q}_l$  which is a linear combination of  $Q_k$  ( $ls \leq k \leq ls+s-1$ ), we have

$$\begin{aligned} q_{i,i+1}(ls) &\leq \tilde{q}_{i,i+1} \leq q_{i,i+1}(ls+s-1), i = 0, 1 \dots S-1, \\ q_{i,S+1}(ls) &\leq \tilde{q}_{i,S+1} \leq q_{i,S+1}(ls+s-1), i = 1, 2 \dots S. \end{aligned}$$

Again, based on the arguments stated before, the reliability in the case of using generator matrix  $\tilde{Q}_l$  must be smaller than that in the case of  $Q_{l_s}$ , while higher than that in the case of  $Q_{l_{s+s-1}}$ . Therefore, the approximation error of reliability by using  $\tilde{Q}_l = \sum_{k=ls}^{ls+s-1} c_k Q_k$  must be smaller than or equal to  $R_2(t) - R_1(t)$ . ■

- Yongkun Li is with the School of Computer Science and Technology, University of Science and Technology of China. (Email: yongkun-lee@gmail.com)
- Patrick P. C. Lee and John C. S. Lui are with the Department of Computer Science and Engineering, The Chinese University of Hong Kong, Hong Kong. (Emails: {pcclee,cslui}@cse.cuhk.edu.hk)

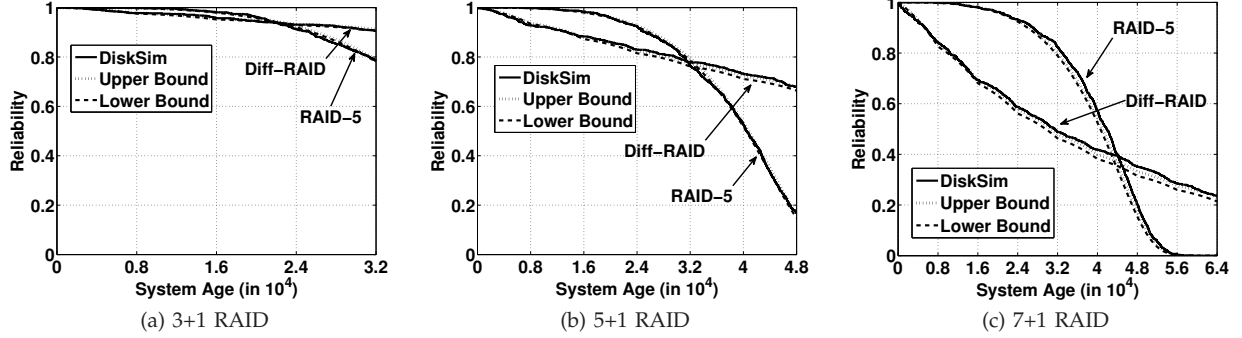


Fig. 2: Model validation with respect to different values of  $N$  ( $c = 0.2 \times 10^{-6}$  and  $\alpha = 2$ ).

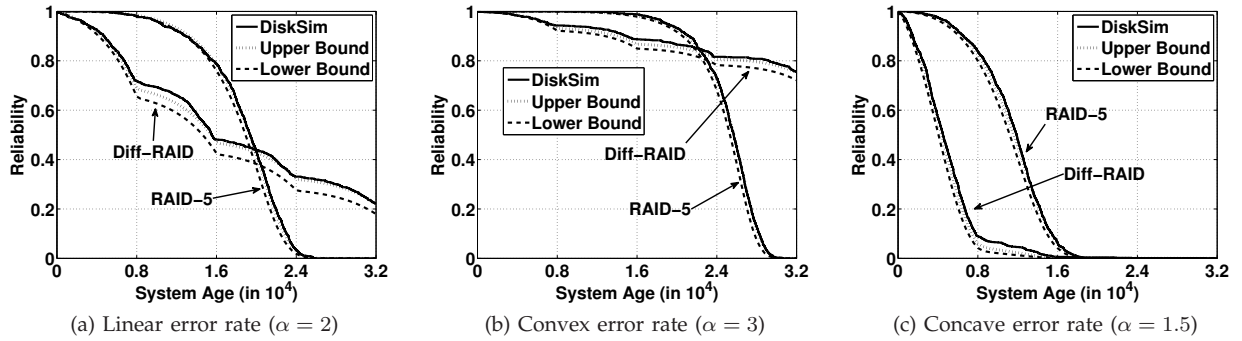


Fig. 3: Model validation with respect to different values of  $\alpha$  ( $N = 3$ ).

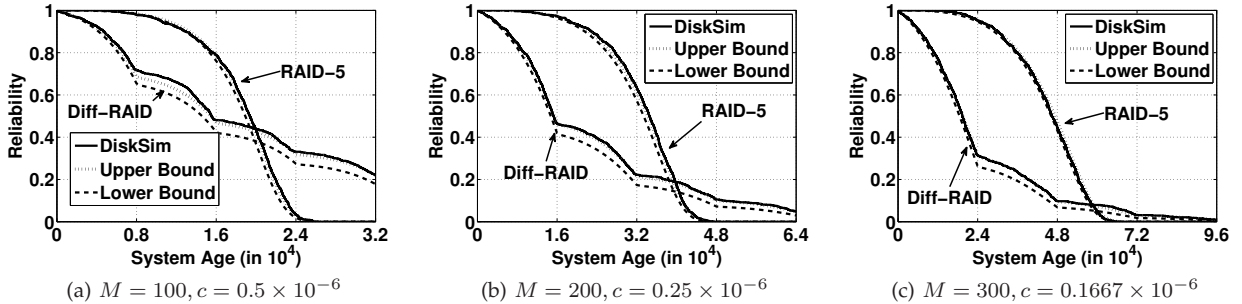


Fig. 4: Model validation with respect to different values of  $M$  ( $N = 3$ ,  $\alpha = 2$ , and  $c\alpha M^{\alpha-1}$  is fixed).

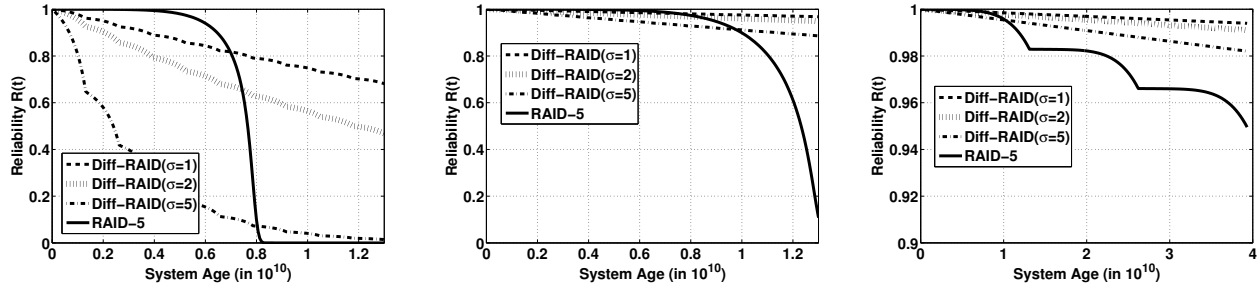
#### 4 MODEL VALIDATION WITH RESPECT TO PARAMETERS $N$ , $\alpha$ AND $M$

In §4.1 of the main paper, we validate our model under different error rates by varying the parameter  $c$ . To complement our work, we also validate our model by varying the parameters  $N$ ,  $\alpha$  and  $M$ . The corresponding parameters are set as follows.

- We validate our model for different system sizes by varying  $N$ . We fix  $c = 0.2 \times 10^{-6}$  and  $\alpha = 2$ . We consider three cases where  $N = 3, 5$ , and  $7$ .
- We validate our model for different error rate functions by varying  $\alpha$ , which determines the change of error rates with respect to the system age. In particular, we consider three cases where  $\alpha = 2, 3$ ,

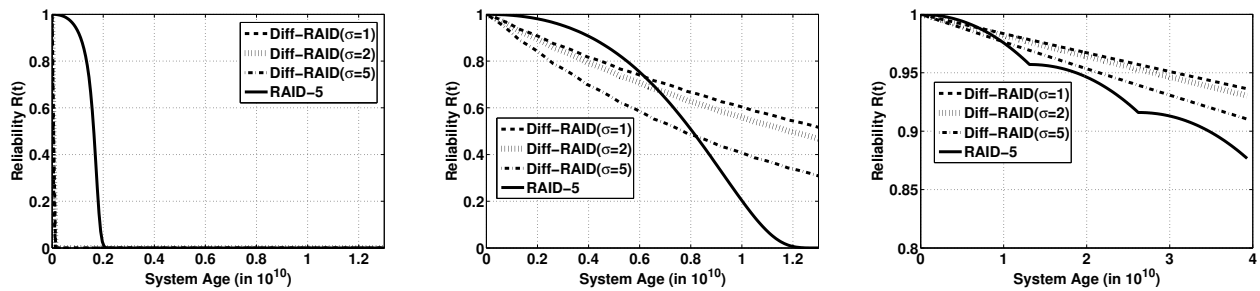
and  $1.5$ , which correspond to the *linear error rate*, *convex error rate*, and *concave error rate*, respectively. We fix the system size by setting  $N = 3$ . To set the parameter  $c$ , note that the maximum error rate in a RAID system may reach  $(N + 1)Sc\alpha M^{\alpha-1}$ . To compare the reliability dynamics under different types of error rates, we fix the maximum error rate instead of the parameter  $c$ . In particular, we set  $c = 0.5 \times 10^{-6}$  when  $\alpha = 2$ , so the maximum error rate is  $(N + 1)Sc\alpha M^{\alpha-1} = 2.048$ . By fixing the maximum error rate, the corresponding values of  $c$  when  $\alpha = 3$  and  $\alpha = 1.5$  can be easily derived, which are  $3.333 \times 10^{-9}$  and  $6.667 \times 10^{-6}$ , respectively.

- We further validate our model for different values of  $M$ . We fix  $N = 3$ ,  $\alpha = 2$ , and vary  $M$  from  $100, 200$



(a) Error dominant case ( $c = 0.73 \times 10^{-17}$ ) (b) Comparable case ( $c = 0.267 \times 10^{-17}$ ) (c) Recovery dominant case ( $c = 0.667 \times 10^{-18}$ )

Fig. 5: Reliability dynamics of SSD arrays (Convex error rate with  $\alpha = 3$ ).



(a) Error dominant case ( $c = 0.147 \times 10^{-10}$ ) (b) Comparable case ( $c = 0.533 \times 10^{-11}$ ) (c) Recovery dominant case ( $c = 0.133 \times 10^{-11}$ )

Fig. 6: Reliability dynamics of SSD arrays (Concave error rate with  $\alpha = 1.5$ ).

to 300. To compare the reliability dynamics under different values of  $M$ , we fix the maximum error rate  $c\alpha M^{\alpha-1}$ . We set  $c = 0.5 \times 10^{-6}$  when  $M = 100$ , so the maximum error rate is  $c\alpha M^{\alpha-1} = 10^{-4}$ . By fixing the maximum error rate, the corresponding values of  $c$  when  $M = 200$  and  $M = 300$  can be easily derived, which are  $0.25 \times 10^{-6}$  and  $0.1667 \times 10^{-6}$ , respectively.

Figures 2, 3 and Figures 4 show the reliability results obtained from the model and simulation for different values of  $N$ ,  $\alpha$ , and  $M$ , respectively. The horizontal axis represents the array age, which denotes the number of erasures performed on the array, and the vertical axis shows the reliability, which denotes the probability of no data loss until the array age reaches at the point indicated by the x-axis. Note that we show the reliability dynamics of a RAID array until all drives wear out once, (i.e., until  $(N + 1)BM$  erasures are performed on the array), so the range of x-axis depends on the array size  $N$ . In particular, Each figure corresponds to one parameter setting, and we show the reliability of both RAID-5 and Diff-RAID. We plot the upper bound and the lower bound obtained from our model, as well as the results with the reliability obtained from the simulator. We observe that the model and simulation results are very close in all cases with different parameters. Thus, our model accurately characterizes the reliability dynamics

of SSD RAID arrays.

## 5 NUMERICAL ANALYSIS ON RELIABILITY DYNAMICS WITH NON-LINEAR ERROR RATE

In §5.2 of the main paper, we study the reliability dynamics of SSD RAID under linear error rate. Here, we show the reliability dynamics in the case of non-linear error rates. We set  $\alpha = 3$  and  $\alpha = 1.5$ , which correspond to the convex and concave error rates, respectively. Other parameters are set according to the description in §5.1 of the main paper. Figures 5 and 6 show the results. We observe similar reliability dynamics as in the case of the linear error rate (see §5.2 of the main paper). Moreover, even for the same maximum error rate, reliability dynamics of SSD RAID system vary a lot for different types of error rates (e.g., linear, convex, and concave). This further shows the importance of capturing the time-varying feature of error rate in SSDs.